

Modeling the Peru Upwelling System seasonal dynamics

Pierrick Penven¹ (penven@univ-brest.fr), Jose Pasapera², Jorge Tam² and Claude Roy¹

¹Institut de Recherche pour le Développement, Plouzané, France & Université de Bretagne Occidentale, Brest, France. ²Instituto del Mar del Perú, Lima, Perú,

The Peru Upwelling System is located along the west coast of South America, approximately between 20°S to 5°S and between 90°W to 70°W, where an equatorward wind forces a strong coastal upwelling. With the Benguela Current System, the Canary Current System and the California Current System, the Peru Upwelling System is one of the four major coastal upwelling regions of the world. These four upwelling systems are highly productive. The Humboldt Current Large Marine Ecosystem (i.e. from the South of Chile to the North of Peru) is the most productive marine ecosystem in the world, as well as the largest upwelling system. It produces approximately 18-20% of the world's fish catch (<http://na.nefsc.noaa.gov/lme/text/lme13.htm>). This production is highly variable and strongly dependent on environmental factors such as sea temperature and currents. In this area, El Niño is a major contributor to environmental variability. In an attempt to investigate the dynamics of the Peru Upwelling System and the coupling between the environment and the ecosystem dynamics, a set of physical and biological models will be implemented. This is part of a joint initiative between IMARPE and IRD. The implementation of the hydrodynamic model and the analysis of its seasonal behaviour presented here are the first steps in the design of a coherent set of numerical tools.

The circulation in the Peru Upwelling System is very complex. Unlike other upwelling systems, the Peru Current System is closely connected to the eastern limit of the equatorial currents (Lukas, 1986). Hence, a model of the Peruvian upwelling should explicitly resolve as well the eastern equatorial dynamics. In this work, the focus is on the average circulation, the seasonal cycle and the mesoscale dynamics of the Peru Current System; the inter-annual variability will be addressed in the near future.

After a presentation of the characteristics of the model, the modeled annual mean circulation is described. Model/data comparisons are then performed as a first test of the ability of our regional configuration to simulate the seasonal cycle in the Peru Upwelling System.

Model characteristics

The ocean model is the Regional Oceanic Modeling System (ROMS). The reader is referred to Shchepetkin and McWilliams (2003) and to Shchepetkin and McWilliams (in press) for a more complete description of the model. ROMS solves the Primitive Equations in an Earth-centered rotating environment, based on the Boussinesq approximation and hydrostatic vertical momentum balance. ROMS is discretized in coastline- and terrain-following curvilinear coordinates. The model grid, forcing, initial and boundary conditions are built using the ROMSTOOLS package (Penven, 2003). To encompass the whole Peru Upwelling System, we have designed a grid extending from 20°S to 3°N and from 90°W to 70°W (Fig. 1) at a resolution of 1/9° (i.e. 10km). The grid contains 192 by 256 points and 32 vertical levels.

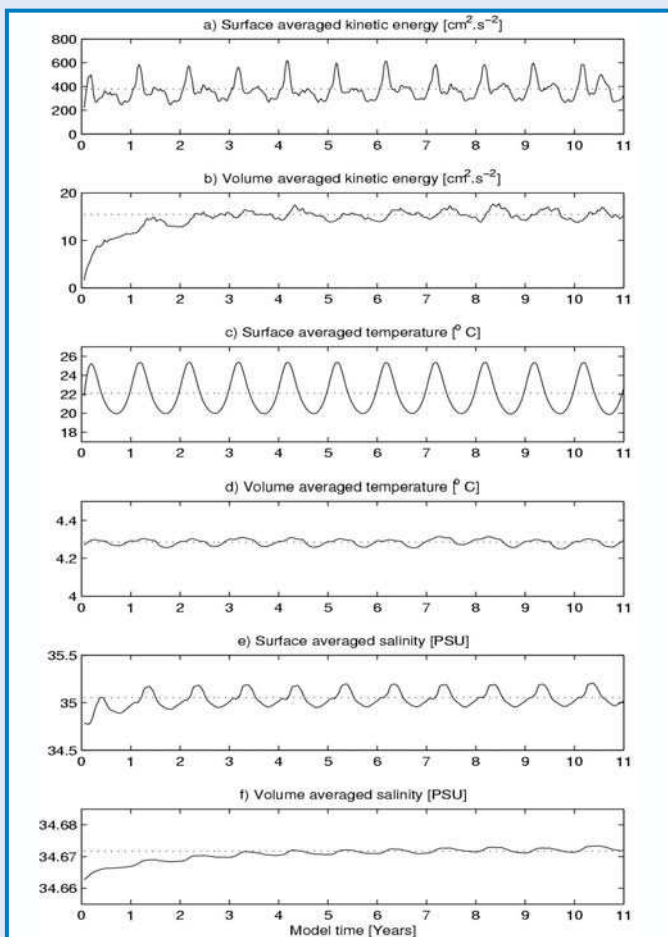


Figure 2. Time evolution of different model variables: a) Surface averaged kinetic energy ($\text{cm}^2.\text{s}^{-2}$), b) Volume averaged kinetic energy ($\text{cm}^2.\text{s}^{-2}$), c) Surface averaged temperature ($^{\circ}\text{C}$), d) Volume averaged temperature ($^{\circ}\text{C}$), e) Surface averaged salinity (PSU), and f) Volume averaged salinity (PSU)

Our modeling procedure is based on a step by step approach. It starts by addressing the mean circulation and seasonal cycle in the Peru Current System, leaving aside the inter-annual variability. The model is forced by COADS ocean surface monthly climatology for the heat and fresh water fluxes, and by a climatology derived from QuickSCAT satellite scatterometer data for the wind stress. The three lateral open boundaries (Marchesiello *et al.*, 2001) are forced using a climatology derived from the OCCAM global ocean model (Saunders *et al.*, 1999).

The model solution reaches a statistical equilibrium after a spin-up of about 2 years. Figure 1 (see page 2) presents a snapshot of the modeled surface currents and sea surface temperature for 8 January of model year 11. One can notice the cold upwelled water along the shore, the upwelling filaments extending from the upwelling front, the equatorward flow along the shore, the offshore Ekman transport, and the strong equator

eastward current. The major ingredients of the known physical dynamics in the region appear to be represented. The cold tongue extending Northwestward from Punta Falsa to the equator is also a typical pattern observed at this time of year. Figure 2 depicts the time variations of surface-averaged kinetic energy (a) volume-averaged kinetic energy (b) surface-averaged temperature (c), volume-averaged temperature (d), surface-averaged salinity (e), and volume-averaged salinity (f). For each of these variables, after a spin-up of 2 years, the model exhibits no significant temporal drift.

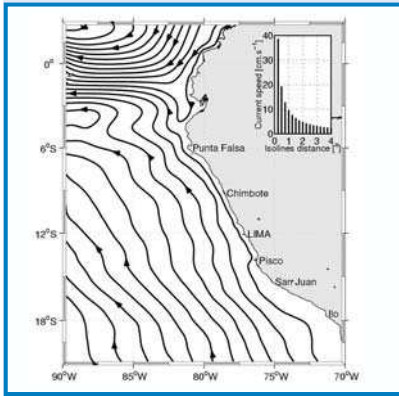


Figure 3. Streamfunction calculated from the annual mean surface velocities. The interval between the isocontours is $10^{-4} \text{ m}^2 \cdot \text{s}^{-1}$. A diagram presenting the distances between the isolines and the corresponding currents speeds is inserted in the upper-right corner

Annual mean circulation

A streamfunction, representative of the nondivergent component of the surface annual mean currents, is derived from the model outputs and portrayed on Figure 3. In this depiction, the principals surface currents described by Lukas (1986) and Strub *et al.* (1998), are represented with a very high degree of realism. In this simulation, the South Equatorial Current is extending from about 2°N to 2°S . It flows westward with velocities in the $25\text{cm}\cdot\text{s}^{-1}$ - $40\text{cm}\cdot\text{s}^{-1}$ range. An important part is fed by a southwest current that is coming from the Northern model boundary. At the western border, around 4°S , a branch of the South Equatorial Counter Current enters the model domain, with velocities of about $10\text{cm}\cdot\text{s}^{-1}$ to $15\text{cm}\cdot\text{s}^{-1}$. At the shore, the Peru Coastal Current is flowing northward following closely the Peruvian coastline, with velocities ranging from $10\text{cm}\cdot\text{s}^{-1}$ to $25\text{cm}\cdot\text{s}^{-1}$. Offshore, in the South-West corner of the model domain, we can detect the presence of the Peru Oceanic Current. From this figure, we can conclude that this simulation gives a most realistic representation of the known ocean surface circulation for this region.

Figure 4 presents a streamfunction calculated from the modeled annual mean velocities at 50m depth. This image shows that already at 50m depth, a poleward undercurrent (the Peru-Chile

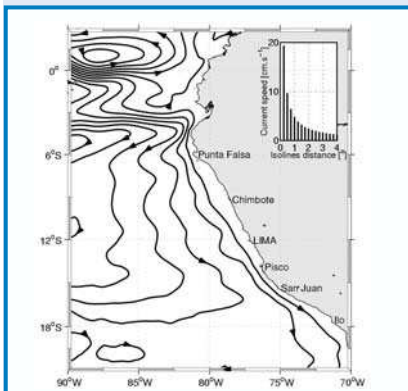


Figure 4. Streamfunction calculated from the annual mean velocities at 50 m depth. The interval between the isocontours is $0.5 \times 10^{-4} \text{ m}^2 \cdot \text{s}^{-1}$. A diagram presenting the distances between the isolines and the corresponding currents speeds is inserted in the upper-right corner.

Under Current) is noticeable at the shore with a speed of about $5\text{cm}\cdot\text{s}^{-1}$ to $15\text{cm}\cdot\text{s}^{-1}$. Part of this flow is fed by the Equatorial Undercurrent (current speed: $20\text{cm}\cdot\text{s}^{-1}$ to $30\text{cm}\cdot\text{s}^{-1}$) and the South Equatorial Undercurrent that enters the model domain at about 4°S with speeds of about $10\text{cm}\cdot\text{s}^{-1}$ to $20\text{cm}\cdot\text{s}^{-1}$. The South Equatorial Undercurrent is also clearly feeding a Peru Subsurface Countercurrent that travels southward at about $5\text{cm}\cdot\text{s}^{-1}$ from a latitude of 6°S . The Peru Subsurface Countercurrent is veering to the left to leave the model domain between 15°S and 18°S . This offshore veering could be a plausible explanation for the termination of the Peru Subsurface Countercurrent.

Seasonal cycle

Being locally forced as well as remotely forced by equatorial variations, the Peru Upwelling system exhibits an important seasonal cycle in sea surface temperature. Figure 5 presents the seasonal variations of sea surface temperature from three different sources: the COADS climatology, our regional model and a climatology derived from Pathfinder AVHRR satellite data. Because COADS sea surface temperature is used as a correction in the model heat fluxes, comparisons between a model forcing (COADS), the model solution, and a more precise dataset (Pathfinder) can help to obtain an evaluation of the model skills.

In summer (Fig. 5a, b and c), the three products show the occurrence of a strong upwelling over the shelf. They all present comparable broadscale patterns: warm water at the equator and colder water in the South. A warm pocket of water is also found around 6°S . Our regional model and Pathfinder are much

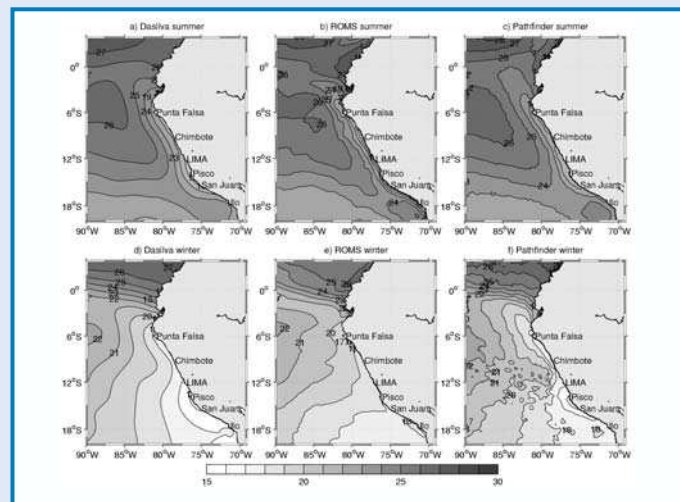


Figure 5. Seasonal variations of sea surface temperature ($^\circ\text{C}$) for the COADS climatology, our regional configuration and a climatology derived from Pathfinder AVHRR satellite data.

similar in their representation of the upwelling front, the cold water tongue extending toward the equator, and the presence of warm water in the southeastern part of the domain. This comparison between model and data suggests that the surface currents simulated by our model adequately compare with reality. The simulation also improves the sea surface temperature patterns, even in comparison to what is used in the model forcing. A few biases are noticeable in our model: the sea surface is slightly too cold close to the shore and a pocket of warm water is present along the Ecuadorian coastline.

In winter, COADS, our model and Pathfinder show the same large scale sea surface temperature pattern (Fig. 5 d, e and f). The position and the width of the equatorial front in the model

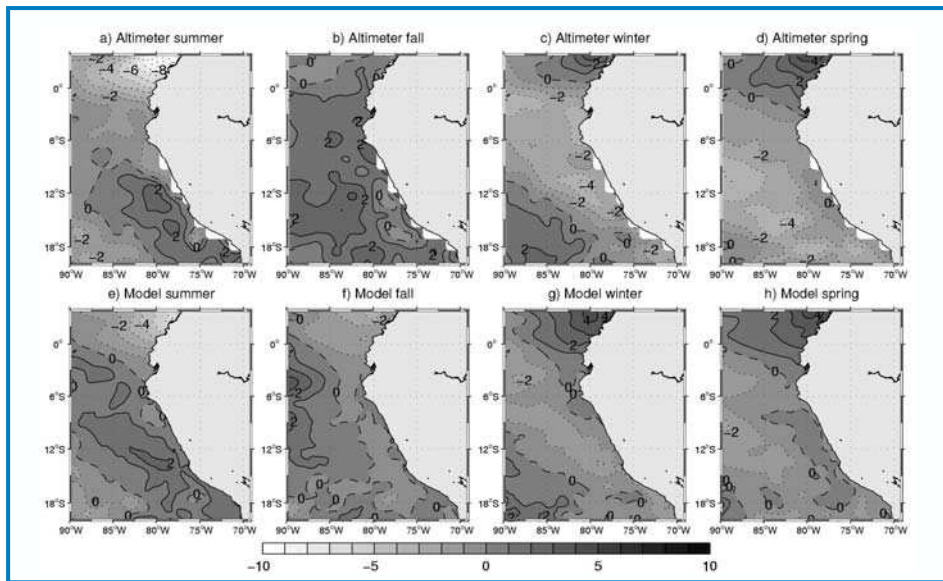


Figure 6. Seasonal mean sea surface height anomalies (cm) for the model simulation and satellite altimeter.

match Pathfinder observations. But, close to the Peruvian coastline, there is still an upwelling for COADS and Pathfinder, a feature that is almost absent in the model simulation. This might be the signature of an important so called El-Niño poleward current that could reduce the upwelling, and/or this also might be associated to weaknesses in local surface forcing.

Seasonal-mean sea surface height anomalies are presented on Figure 6 for both the model simulation and satellite altimeter. Altimeter measurements come from high-resolution merged TOPEX/Poseidon and ERS-1 and -2 data (Ducet *et al.*, 2000). The simulated and observed sea surface height anomalies are relatively similar in their patterns. In the northern part of the domain, a strong seasonal oscillation is noticeable in both model and observations. It gets a minimum value of -10cm for the satellite (Fig. 6a) and -6 cm for the model (Fig. 6e) in summer, and a maximum value of 4 cm for both model and altimeters in winter and spring. For the Central Peru Upwelling System, in summer, a large (about 1000km) anticyclone, centered at about 12°S and 80°W, showing a 2cm maximum of anomaly in sea surface height, is present in both altimeter and model solutions (Fig. 6a and e). The seasonal geostrophic current anomaly is thus south-westward, with strong similarities for each product, in summer in the south-east corner of the domain. A first signature of this anticyclonic structure is noticeable along the Peruvian shore in spring (Fig. 6d and h). This pattern is reversed in winter, and the seasonal geostrophic current anomaly in the south-east corner of the domain is now directed toward the north-east for the model and altimeter (Fig. 6c and g).

This comparison between data and simulated fields gives us confidence in the model ability to adequately reproduce surface oceanic patterns as well as the large scale surface circulation in the Peru Current System. A few biases such as the weakness of upwelling in winter, are still present and will be addressed in the near future.

Conclusion

In this short note, the implementation and first tests of a high resolution model of the Peru Upwelling System are presented. The model domain encompasses both the Upwelling System and the equatorial current area; thus the equatorial influence on the

Peru Upwelling System is explicitly resolved. The simulated surface and subsurface annual mean circulation patterns seem to be in agreement with the known dynamics of the region. For the seasonal cycle, our regional configuration compares well with Pathfinder AVHRR sea surface temperature data and with altimeter data. Further analysis of this simulation will be conducted to gain more insights on the Peru Upwelling System dynamics. This model could then be used to conduct inter-annual simulations, such as El-Niños or inter-decadal variations.

At IMARPE, this model is currently coupled to an ecosystem model to simulate the primary and secondary production patterns. We also expect to use the model outputs to conduct an analysis of the Lagrangian transport patterns in this area. These studies will be used at a later stage to gain insight on fisheries and marine resources related questions, such as fish eggs and larvae transport.

Acknowledgments

QuickSCAT data were obtained from the NASA / NOAA Seaflux, courtesy of W. Liu and Tang. OCCAM data were obtained from the courtesy of C. Coward. Altimeter data were prepared by Ramos, PROFCA, Concepcion, Chile. Support for this study is provided by the IDYLE research unit from IRD/France and by CIMOBP/IMARPE. This is a contribution to GLOBEC-SPACC.

References

- Ducet, N., P.Y.L. Traon, and G. Reverdin. 2000. Global high-resolution mapping of ocean circulation from TOPEX/Poseidon and ERS-1 and -2. *Journal of Geophysical Research* 105: 19,477-19,498.
- Lukas, R. 1986. The termination of the equatorial undercurrent in the eastern Pacific. *Progress in Oceanography* 16: 63-90, 1986.
- Marchesiello, P., J.C. McWilliams, and A. Shchepetkin. 2001. Open boundary condition for long-term integration of regional oceanic models. *Ocean Modelling* 3: 1-21.
- Penven, P., ROMSTOOLS user's guide (http://fraise.univ-brest.fr/penven/roms_tools/). *IRD Technical Report*.
- Saunders, P.M., A.C. Coward, and B.A. de Cuevas. 1999. Circulation of the Pacific Ocean seen in a global ocean model (OCCAM). *Journal of Geophysical Research* 108: 18,281-18,299.
- Shchepetkin, A.F., and J.C. McWilliams. 2003. A method for computing horizontal pressure-gradient force in an ocean model with a non-aligned vertical coordinate, *Journal of Geophysical Research* 108(C3): article no: 3090.
- Shchepetkin, A.F., and J.C. McWilliams. In press. Regional Ocean Model System: a split-explicit ocean model with a free-surface and topography-following vertical coordinate. *Journal of Computational Physics*.
- Strub, P.T., J.M. Mesias, V. Montecino, J. Rutllant, and S. Salinas. 1998. Coastal ocean circulation off western South America. In: Robinson, A.R. and K.R. Brink. (editors). *The Sea*, vol. 11. John Wiley and Sons, p.273-314.

Ice, Bloom, and Copepods

Early Ice Retreat → Late Bloom, Warm Water - Large Copepod Biomass



Late Ice Retreat → Early Bloom, Cold Water - Small Copepod Biomass



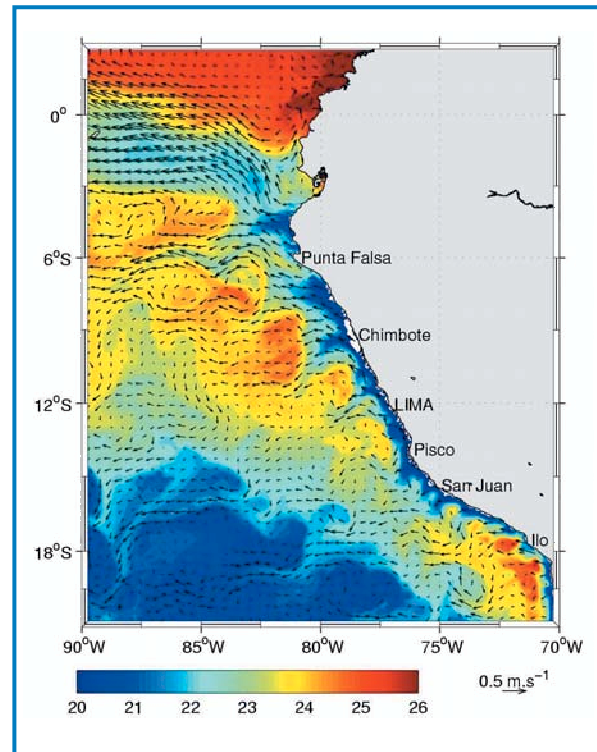
February March April May June

Figure 1. (Hunt, p. 30 -31) The relationship between the timing of sea ice retreat and the timing and fate of the bloom. Top: If the ice retreats in mid-March or earlier, the bloom is delayed until insolation warms and stratifies the water column. The bloom then occurs in warm water and is more strongly coupled to zooplankton grazing. Bottom: If ice retreat is delayed into late-March or April, there will be an ice-associated bloom in cold water that is decoupled from copepod grazing. Full article on pages 30 - 31.

Figure 1. (Penven, p. 23 - 25) An example of modeled surface currents (1 vector every 4 grid points) and sea surface temperature (°C) for the 8 January of model year 11. Full article on p. 23 -25.

SPACC Workshop on the economics of small pelagics and climate change. University of Portsmouth, Portsmouth, UK. September 2004.

The focus of the workshop is on the economic implications of small pelagic fish fluctuations. We are looking both for papers that are backward looking and theoretical or forward looking. Abstracts should be sent to the GLOBEC IPO through its webpage (www.globec.org, follow signs to "SPACC Economics Workshop") by February 29, 2004. Authors of accepted papers will be invited and sponsored. It is expected to publish the papers presented at the conference as a special volume of a relevant journal or as a book of case studies.



GLOBEC INTERNATIONAL

GLOBEC International Newsletter is published biannually by the GLOBEC International Project Office, Plymouth UK. Correspondence may be directed to the IPO at the address below or by e-mail on: globec@pml.ac.uk. Articles, contributions and suggestions are welcome. To subscribe to GLOBEC International Newsletter, or to change your mailing address, please use the same address. GLOBEC International Project Office, Plymouth Marine Laboratory, Prospect Place, West Hoe, Plymouth, PL1 3DH, United Kingdom.

Tel: (01752) 633401, Fax (01752) 633101, <http://www.globec.org>

Printed on 100% recycled paper, Revived Matt 130g/m²

Circulation: 1600

Editor: Manuel Barange (Director, GLOBEC IPO)



Produced by: Pepper Communications Tel: (01752) 348800